Pin-wise homogenization for SP_N neutron transport approximation using the finite element method

A. Vidal-Ferràndiz[a], S. González-Pintor[b], D. Ginestar[d,*], C. Demazière[c], G. Verdú[a]

[a] *Instituto de Seguridad Industrial: Radiofísica y Medioambiental, Universitat Politècnica de València, Camino de Vera s/n, 46022, València, Spain*
[b] *Department of Mathematical Sciences Chalmers University of Technology and the University of Gothenburg, SE-41296 Gothenburg, Sweden*
[c] *Subatomic and Plasma Physics, Department of Physics Chalmers University of Technology, SE-41296, Göteborg, Sweden*
[d] *Instituto Universitario de Matemática Multidisciplinar, Universitat Politècnica de València, Camino de Vera s/n, 46022, València, Spain*

Abstract

The neutron transport equation describes the distribution of neutrons inside a nuclear reactor core. Homogenization strategies have been used for decades to reduce the spatial and angular domain complexity of a nuclear reactor by replacing previously calculated heterogeneous subdomains by homogeneous ones and using a low order transport approximation to solve the new problem. The generalized equivalence theory for homogenization looks for discontinuous solutions through the introduction of discontinuity factors at the boundaries of the homogenized subdomains. In this work, the generalized equivalence theory is extended to the Simplified P_N equations using the finite element method. This extension proposes pin discontinuity factors instead of the usual assembly discontinuity factors and the use of the simplified spherical harmonics approximation rather than diffusion theory. An interior penalty finite element method is used to discretize and solve the problem using discontinuity factors. One dimensional numerical results show that the proposed pin discontinuity factors produce more accurate results than the usual assembly discontinuity factors. The proposed pin discontinuity factors produce precise results for both pin and assembly averaged values without using advanced reconstruction methods. Also, the homogenization methodology is verified against the calculation performed with reference discontinuity factors.

Keywords: Homogenization, Finite Element Method, Discontinuous Galerkin, SP_N equations.

*Corresponding author
Email addresses: anvifer2@upv.es (A. Vidal-Ferràndiz), sebastian.gonzalez-pintor@chalmers.se (S. González-Pintor), dginesta@mat.upv.es (D. Ginestar), demaz@chalmers.se (C. Demazière), gverdu@iqn.upv.es (G. Verdú)

1. Introduction

The neutron transport equation describes the distribution of neutrons inside a nuclear reactor core and its dynamics. Many different methods have been used to approximate this equation, and the integro-differential formulation is studied here [1]. In particular, the steady-state distribution satisfies an integro-differential eigenvalue problem, and its solution is fundamental because it is used as initial condition for the time dependent simulations. The steady-state problem is also important because it gives a measure of the criticality of the reactor.

Many different schemes have been employed to discretize the neutron transport equation with respect to the angular variable [1], as the Discrete Ordinates method (S_N) or the Spherical Harmonics (P_N); and with respect to the spatial variable, such as the Finite Differences (FD), the Finite Element Method (FEM) [2], the Finite Volume Method (FVM) and different derivations of nodal methods. These methods perform differently depending on the problem, but, in general, they all require similar computational resources to achieve similar accuracy. Thus, the problem remains computationally challenging because of the complexity of the spatial domain and the fine angular discretization required to accurately solve it. To reduce computational cost, this problem is usually solved with a scheme consisting of two stages of calculation for different scales through a homogenization process [3].

Spatial homogenization consists in replacing heterogeneous subdomains by homogeneous ones, in such a way that the homogenized problem provides fast and accurate average results. Because the homogenized function to be calculated is smoother than the heterogeneous one, the original exact transport operator can be replaced with a low-order transport operator that eliminates some of the complexity of the original problem. In this way, the global solution can be reconstructed approximately using the previously computed isolated heterogeneous subdomain solutions multiplied by the average values of the subdomain obtained from the homogenized problem over the whole domain.

A first step in a homogenization methodology is to choose heterogeneous reactor properties that should be reproduced when the homogenized problem is solved. Usually, these quantities are the subdomain averaged reaction rates, the surface-averaged net currents and the multiplicative constant of the reactor, which is implicitly conserved if the two aforementioned quantities are preserved. In the generalized equivalence theory [4], which is an extension of Koebke's homogenization method [5], flux discontinuity factors are introduced, relaxing the condition of continuity of the neutron flux on the interior faces of the homogenized regions. Different homogenization strategies and definitions of discontinuity factors exist, such as the flux discontinuity ratios [6], the current discontinuity factors [3] or the consistent discontinuity factors with the reconstruction method [7], among others. Also, different mathematical justifications of the homogenization process in periodic lattices have been developed [8, 9].

For nuclear systems, spatial homogenization makes use of the periodicity of the geometry of a nuclear core. A nuclear core consists of around 150-700 fuel assemblies measuring from 10 cm to 30 cm in radial size and slightly less than 4 m axially. Also, each of the fuel assemblies is constituted by typically hundreds of solid fuel pins containing fissile nuclei surrounded by a thin layer of water. Even though each assembly and pin contain different nuclear enrichments, they have the same geometry and similar neutron flux behaviour [10].

For a long time, the preferred low order operator used for whole core calculations has been the neutron diffusion equation and the homogenized regions have been subdomains of the size of a fuel assembly. Because the computational resources available have increased, the homogenized regions have decreased to the size of a single pin and the low order operator relying on

diffusion theory is being abandoned so that transport effects that occur at these smaller scales can be taken into account. One could for instance use the Simplified P_N (SP_N) formulation [11]. Homogenization errors for pin computations are the main concern in these approximations, and they have been recently studied for different problems [12, 13]. The main issue has been the definition of the discontinuity factors for the SP_N approximation in two- or three-dimensional problems [14, 15, 16, 17]. On the other hand, the SP_N approximation has been implemented using the finite element method (FEM) for the spatial discretization [18, 19, 20].

In this work, we focus on the implementation of the classical discontinuity factors for the correction of the homogenization error in a FEM when using SP_N as low order operator for pin-wise homogenization in one-dimensional problems, where the ambiguity in the definition of the flux discontinuity factors does not exist. It must be noted that one dimensional SP_N approximation is equivalent to the complete P_N approximation. We quantify the error of the proposed pin discontinuity factors and compare it to the usual assembly-wise homogenization.

The rest of the paper is structured as follows. In Section 2, we introduce the transport equation and the angular approximations that are relevant for this work, together with the spatial discretization with the Interior Penalty Finite Element Method (IP-FEM). The homogenization technique is briefly presented in Section 3 together with the discontinuity factors definition and the way they are introduced in the Interior Penalty Finite Element Method. In Section 4, we test the performance of the SP_N neutron transport approximation using one-dimensional problems against the SP_N solution with IP-FEM without discontinuity factors, and against the classical diffusion theory with discontinuity factors in order to show the importance of using discontinuity factors for the homogenized equation. We finish with a brief summary and some conclusions regarding the present study in Section 5.

2. The one-dimensional Simplified P_N equations and their discretization

We consider the eigenvalue problem associated with the steady-state, multi-group, linear Boltzmann transport equation [21], in slab geometry,

$$\left(\mu\frac{\mathrm{d}}{\mathrm{d}x}+\Sigma_t^g(x)\right)\psi^g(x,\mu)=\sum_{g'=1}^{G}\int_{-1}^{1}\Sigma_s^{gg'}(x,\mu_0)\psi^{g'}(x,\mu')\mathrm{d}\mu'+\frac{1}{\lambda}\sum_{g'=1}^{G}\frac{\chi^g(x)}{2}\nu\Sigma_f^{g'}(x)\int_{-1}^{1}\psi^{g'}(x,\mu')\mathrm{d}\mu',$$
$$g=1,\ldots,G,\qquad x\in[0,\,L_t] \tag{1}$$

with vacuum boundary conditions at the extremes of the domain, $x = 0$ and $x = L_t$

$$\psi^g(0,\mu_{in})=0,\qquad \psi^g(L_t,\mu_{in})=0. \tag{2}$$

G is the number of groups of energy considered, θ is the angle between the direction of the incident neutron velocity and the x axis, $\mu = cos(\theta)$, θ_0 is the angle between the incident neutrons and the scattered neutrons, $\mu_0 = cos(\theta_0)$. μ_{in} is the set of directions cosines that are incident at a given boundary, in other words, at $x = 0$, $0 < \mu \leq 1$ and at $x = L_t$, $-1 \leq \mu < 0$. Other quantities of interest are given in Table 1. The solutions of this eigenvalue problem are known as the Lambda Modes of the transport equation [22]. The dominant eigenvalue, $\lambda = k_{\mathrm{eff}}$, is the multiplicative factor of the system and measures its criticality and the corresponding eigenvector is the stationary angular flux distribution inside the domain.

Table 1: Definition of the different quantities involved in Boltzmann's neutron transport equation.

$\psi^g(x,\mu)$	Angular flux for group g and eigenvector of the problem.
λ	Eigenvalue value of the problem.
$\Sigma_t^g(x)$	Total cross section for group energy g.
$\Sigma_s^{gg'}(x,\mu_0)$	Scattering cross section through angle $\mu_0 = cos(\theta_0)$ from group g' to g.
$\nu\Sigma_f^{g'}(x)$	Fission cross section for energy group g' multiplied by the average number of neutrons per fission.
$\chi^g(x)$	Energy fission spectrum for group energy g.

Different angular discretizations are commonly used to solve this problem, as the discrete ordinates or the spherical harmonics expansion of the angular variable. In one-dimensional geometries, both discretizations provide equivalent solutions with an appropriate choice of the quadrature set that defines the discrete ordinates method, [23], and have simplified second order forms, where odd moments are formally solved and substituted back into the equations, providing a simplified formulation where the number of unknown fields is reduced.

The SP_N approximation, which is the subject of study of this work, generally does not converge to the true transport solution when $N \to \infty$, except in one-dimensional problems where it is equivalent to the complete P_N approximations. Nevertheless, it is used as a low order approximation of the neutron transport equation for coarse meshes. After a homogenization process of the domain in coarser structures, transport effects are less important and this approximation is enough to capture the coarse scale behaviour of the transport equation. In this work, the spherical harmonics order is increased as far as 5. Higher orders do not produce better results for homogenized full-core problems as the homogenization error is greater than the angular discretization error [24]. This work only deals with odd order SP_N approximations because they have found broader acceptance.

2.1. Simplified P_N Angular Discretization

The P_N approximation to the neutron transport equation (1) assumes that the angular dependence of both the angular neutron flux distribution and the scattering cross-section can be expanded in terms of $N+1$ Legendre polynomials, $P_n(\mu)$, where N is odd in this work, as

$$\psi^g(x,\mu) = \sum_{n=0}^{N} \frac{2n+1}{2} \phi_n^g(x) P_n(\mu), \tag{3}$$

$$\Sigma_s^{gg'}(x,\mu_0) = \sum_{n=0}^{L} \frac{2n+1}{2} \Sigma_{sn}^{gg'}(x) P_n(\mu_0) . \tag{4}$$

where ϕ_n^g are the angular moments of the neutron flux, and $\Sigma_{sn}^{gg'}$ are the scattering cross sections moments up to order $L \leq N$. Using expansions (3) and (4) into equation (1) and employing the orthogonality relations for these polynomials, the following P_N approximation equations are

obtained [25],

$$\frac{\mathrm{d}\phi_1^g}{\mathrm{d}x} + \sum_{g'=1}^{G}\left(\Sigma_t^g - \Sigma_{s0}^{gg'}\right)\phi_0^{g'} = \frac{1}{\lambda}\sum_{g'=1}^{G}\chi^g\nu\Sigma_f^{g'}\phi_0^{g'}, \tag{5}$$

$$\frac{\mathrm{d}}{\mathrm{d}x}\left(\frac{n}{2n+1}\phi_{n-1}^g + \frac{n+1}{2n+1}\phi_{n+1}^g\right) + \sum_{g'=1}^{G}(\delta_{gg'}\Sigma_t^g - \Sigma_{sn}^{gg'})\phi_n^{g'} = 0, \qquad \text{for } n = 1,\ ....,\ N. \tag{6}$$

where we consider the expansion order for the angular flux, N, to be larger than the order of anisotropic scattering, L. In this formulation, we consider the components of the scattering equal to zero for moments higher than L, but we keep them in the formulation for simplicity. The P_N equations (5) and (6) constitute a set of $N+1$ equations with $N+2$ unknowns. This problem is usually solved setting the derivative of the highest order moment to zero $\frac{\mathrm{d}}{\mathrm{d}x}\phi_{N+1} = 0$. This closure is the most common and straightforward but can be problematic for some time dependent applications, so other closures have also been developed [26].

Equations (5) and (6) are more easily expressed in matrix notations as,

$$\frac{\mathrm{d}\,\Phi_1}{\mathrm{d}x} + \mathbf{\Sigma_0}\Phi_0 = \frac{1}{\lambda}\mathbf{F}\Phi_0\,, \tag{7}$$

$$\frac{\mathrm{d}}{\mathrm{d}x}\left(\frac{n}{2n+1}\Phi_{n-1} + \frac{n+1}{2n+1}\Phi_{n+1}\right) + \mathbf{\Sigma_n}\Phi_n = 0\,, \qquad \text{for } n = 1,\ ....,\ N. \tag{8}$$

where,

$$\mathbf{\Sigma_n} = \begin{pmatrix} \Sigma_t^0 - \Sigma_{sn}^{00} & -\Sigma_{sn}^{01} & \dots & -\Sigma_{sn}^{0G} \\ -\Sigma_{sn}^{10} & \Sigma_t^1 - \Sigma_{sn}^{11} & \dots & -\Sigma_{sn}^{1G} \\ \vdots & \vdots & \ddots & \vdots \\ -\Sigma_{sn}^{G0} & -\Sigma_{sn}^{G1} & \dots & \Sigma_t^G - \Sigma_{sn}^{GG} \end{pmatrix},\ \mathbf{F} = \begin{pmatrix} \chi^0\nu\Sigma_f^0 & \chi^0\nu\Sigma_f^1 & \dots & \chi^0\nu\Sigma_f^G \\ \chi^1\nu\Sigma_f^0 & \chi^1\nu\Sigma_f^1 & \dots & \chi^1\nu\Sigma_f^G \\ \vdots & \vdots & \ddots & \vdots \\ \chi^G\nu\Sigma_f^0 & \chi^G\nu\Sigma_f^1 & \dots & \chi^G\nu\Sigma_f^G \end{pmatrix},$$

$$\Phi_n = \left(\phi_n^1, \phi_n^2, \dots, \phi_n^G,\right)^T\,.$$

It must be noted that in many nuclear applications, as in usual static reactor calculations, the scattering cross section, Σ_s, is considered isotropic and a transport correction is typically introduced [27]. Thus, considering isotropic scattering, i.e. $L = 0$ in equation (4), the matrix $\mathbf{\Sigma_n}$ is diagonal for $n > 0$. Substituting the equations related to the odd moments of the flux, equation (8) yields

$$-\frac{\mathrm{d}}{\mathrm{d}x}\left(\frac{n\mathbf{\Sigma_{n-1}}^{-1}}{(2n+1)(2n-1)}\frac{\mathrm{d}}{\mathrm{d}x}\left((n-1)\Phi_{n-2} + n\Phi_n\right) + \frac{(n+1)\mathbf{\Sigma_{n+1}}^{-1}}{(2n+1)(2n+3)}\frac{\mathrm{d}}{\mathrm{d}x}\left((n+1)\Phi_n + (n+2)\Phi_{n+2}\right)\right)$$
$$+ \mathbf{\Sigma_n}\Phi_n = \frac{1}{\lambda}\mathbf{F}\Phi_n\delta_{n0}, \qquad \text{for } n = 2,\ 4,\ \dots,\ N. \tag{9}$$

Equation (9) defines an eigenvalue problem associated with a linear system of $(N+1)/2$ elliptic, second-order equations. This eigenvalue problem can be converted into a problem composed of a set of diffusion-like equations if the following linear change of variables is preformed,

$$U_n = (n+1)\,\Phi_n + (n+2)\,\Phi_{n+2}, \quad n = 0,\ 2,\ \dots,\ N-1, \tag{10}$$

$$U = (U_0,\ U_2,\ \dots,\ U_{N-1})^T\,, \tag{11}$$

and each element of U contains the group dependent diffusive moments

$$U_n = (u_n^1, u_n^2, \ldots, u_n^G)^T \,. \tag{12}$$

For example, the set of P_5 equations are

$$\begin{aligned}
-\frac{\mathrm{d}}{\mathrm{d}x}\left(\frac{1}{3}{\boldsymbol{\Sigma_1}}^{-1}\frac{\mathrm{d}}{\mathrm{d}x}\left(\Phi_0+2\Phi_2\right)\right)+\boldsymbol{\Sigma_0}\Phi_0 &= \frac{1}{\lambda}\mathbf{F}\Phi_0\,,\\
-\frac{\mathrm{d}}{\mathrm{d}x}\left(\frac{2}{15}{\boldsymbol{\Sigma_1}}^{-1}\frac{\mathrm{d}}{\mathrm{d}x}\left(\Phi_0+2\Phi_2\right)+\frac{3}{35}{\boldsymbol{\Sigma_3}}^{-1}\frac{\mathrm{d}}{\mathrm{d}x}\left(3\Phi_2+4\Phi_4\right)\right)+\boldsymbol{\Sigma_2}\Phi_2 &= 0\,,\\
-\frac{\mathrm{d}}{\mathrm{d}x}\left(\frac{4}{63}{\boldsymbol{\Sigma_3}}^{-1}\frac{\mathrm{d}}{\mathrm{d}x}\left(3\Phi_2+4\Phi_4\right)+\frac{5}{99}{\boldsymbol{\Sigma_5}}^{-1}\frac{\mathrm{d}}{\mathrm{d}x}\left(5\Phi_4+6\Phi_6\right)\right)+\boldsymbol{\Sigma_4}\Phi_4 &= 0\,,
\end{aligned} \tag{13}$$

Using the change of variables,

$$U_0 = \Phi_0 + 2\Phi_2\,, \quad U_2 = 3\Phi_2 + 4\Phi_4\,, \quad U_4 = 5\Phi_4 + 6\Phi_6\,, \tag{14}$$

the system (13) is rewritten as the eigenvalue problem,

$$-\frac{\mathrm{d}}{\mathrm{d}x}\left(\mathbf{D}\frac{\mathrm{d}}{\mathrm{d}x}U\right)+\mathbf{A}U = \frac{1}{\lambda}\mathbf{M}U\,, \tag{15}$$

where the effective diffusion matrix, $\mathbf{D}$, the absorption matrix, $\mathbf{A}$, and the fission matrix, $\mathbf{M}$, are defined as,

$$\mathbf{D} = \begin{pmatrix} \frac{1}{3}{\boldsymbol{\Sigma_1}}^{-1} & 0 & 0 \\ 0 & \frac{1}{5}{\boldsymbol{\Sigma_3}}^{-1} & 0 \\ 0 & 0 & \frac{1}{7}{\boldsymbol{\Sigma_5}}^{-1} \end{pmatrix}, \quad \mathbf{A}_{ij} = \sum_{n=1}^{3}\mathbf{c}_{ij}^{(\mathbf{n})}\boldsymbol{\Sigma}_{\mathbf{n}}\,, \quad \mathbf{M}_{ij} = \mathbf{c}_{ij}^{(\mathbf{1})}\mathbf{F}\,, \tag{16}$$

and the coefficients matrix, $\mathbf{c}^{(\mathbf{m})}$,

$$\mathbf{c}^{(\mathbf{1})} = \begin{pmatrix} 1 & -\frac{2}{3} & \frac{8}{15} \\ -\frac{2}{3} & \frac{4}{9} & -\frac{16}{45} \\ -\frac{8}{15} & -\frac{16}{45} & \frac{64}{225} \end{pmatrix}, \quad \mathbf{c}^{(\mathbf{2})} = \begin{pmatrix} 0 & 0 & 0 \\ 0 & \frac{5}{9} & -\frac{4}{9} \\ 0 & -\frac{4}{9} & \frac{16}{45} \end{pmatrix}, \quad \mathbf{c}^{(\mathbf{3})} = \begin{pmatrix} 0 & 0 & 0 \\ 0 & 0 & 0 \\ 0 & 0 & \frac{9}{25} \end{pmatrix}. \tag{17}$$

For details about the derivation of the boundary conditions, the reader is referred to Appendix A.

For multidimensional problems, the SP_N approximation is obtained substituting the x derivative gradient operator by the corresponding two- or three-dimensional gradient operator in equation (7) and equation (8). These equations are much simpler than the multidimensional P_N equations and can be easily implemented using numerical methods suited for diffusion-like equations.

2.2. Spatial discretization using the Interior Penalty-Finite element method

For the spatial discretization of the diffusive eigenvalue problem corresponding to equation (15), a Discontinuous Galerkin finite element method is used extending the method presented in [28] for the SP_N equations. If discontinuity factors are not taken into account, the interior penalty finite element element method can be formulated as follows. First, we choose a

partition of the one-dimensional domain, $\mathcal{I}_h$, resulting in a splitting of the original domain defining the reactor, Ω, into subdomains, $I_k = [e_{k-1}, e_k]$, $k = 1 \ldots, N_k$, defining the mesh. Second, we define $\mathcal{E}_h := \mathcal{E}_h^0 \cup \mathcal{E}_h^\partial$, as the set of all points that define the partition into subintervals, including the boundaries of the domain $\mathcal{E}_h^\partial := \{e_0, e_{N_k}\}$, and the interior interfaces $\mathcal{E}_h^0 := \{e_k,\ k = 1, \ldots, N_k - 1\}$. Now, problem (15) together with the continuity conditions for the moments and its derivatives, considering zero Dirichlet boundary conditions for clarity (for different boundary conditions, as the ones shown in Appendix A, see [28]), can be rewritten in a generic form, as

$$-\frac{\mathrm{d}}{\mathrm{d}x} \cdot D_n \frac{\mathrm{d}}{\mathrm{d}x} u_n + \Sigma\, u_n = q_n \quad \text{in each } I_k \in \mathcal{I}_h\,, \tag{18}$$

$$[\![u_n(e)]\!] = 0 \quad \text{on each } e \in \mathcal{E}_h\,, \tag{19}$$

$$\left[\!\!\left[D_n \frac{\mathrm{d}}{\mathrm{d}x} u_n(e) \right]\!\!\right] = 0 \quad \text{on each } e \in \mathcal{E}_h^0\,. \tag{20}$$

where the jumps $[\![\cdot]\!]$ are defined by

$$\begin{aligned} [\![u_n]\!] &= \mathbf{n}^- u_n^- + \mathbf{n}^+ u_n^+ = u_n^- - u_n^+, \text{ on } e \in \mathcal{E}_h^0, \\ [\![u_n]\!] &= \begin{cases} \mathbf{n}^+ u_n^+(e_0) & = -u_n^+(e_0) \\ \mathbf{n}^- u_n^-(e_{N_k}) & = +u_n^-(e_{N_k}) \end{cases}, \text{ on } e \in \mathcal{E}_h^\partial, \end{aligned} \tag{21}$$

where $u_n^\pm$ are the lateral limits of u_n in a particular node, and $\mathbf{n}^\pm$ are the normal vectors outward to the adjacent cells $-$ and $+$ at the shared node e, so $\mathbf{n}^- = +1$ and $\mathbf{n}^+ = -1$ in one-dimension. The indices for energy group g are avoided for simplicity of the notation, considering all the contributions coming from different energy and moments inside the source term q_n, together with the neutrons produced due to the fission terms. Standard Interior Penalty Finite Element Methods (IP-FEM) exist for the previous problem as follows [29]:

Find $u_n \in \mathrm{H}^1(\mathcal{I}_h)$ such that

$$\left(D_n \frac{\mathrm{d}}{\mathrm{d}x} u_n, \frac{\mathrm{d}}{\mathrm{d}x} v \right)_{\mathcal{I}_h} + (\Sigma u_n, v)_{\mathcal{I}_h} - \left(\left\{ D_n \frac{\mathrm{d}}{\mathrm{d}x} u_n \right\}, [\![v]\!] \right)_{\mathcal{E}_h} + (s_1 [\![u_n]\!], [\![v]\!])_{\mathcal{E}_h} = (q_n, v)_{\mathcal{I}_h},\ \forall v \in \mathrm{H}^1(\mathcal{I}_h)\,, \tag{22}$$

where $\mathrm{H}^1(\mathcal{I}_h) := \left\{ v \in \mathrm{L}^2(\Omega) : \quad v_{|I_k} \in \mathrm{H}^1(I_k) \quad \forall I_k \in \mathcal{I}_h \right\}$, s_1 is a penalty parameter large enough to stabilize the problem, the averages $\{\cdot\}$ are defined by

$$\{u\} = \frac{1}{2}(u^- + u^+), \text{ on } e \in \mathcal{E}_h^0, \quad \{u\} = u, \text{ on } e \in \mathcal{E}_h^\partial. \tag{23}$$

Alternatively, using the edge operators over interior points, the problem can be rewritten as:
Find $u_n \in \mathrm{H}^1(\mathcal{I}_h)$ such that

$$\begin{aligned} &\left(D_n \frac{\mathrm{d}}{\mathrm{d}x} u_n, \frac{\mathrm{d}}{\mathrm{d}x} v \right)_{\mathcal{I}_h} + (\Sigma u_n, v)_{\mathcal{I}_h} - \left(\left\{ D_n \frac{\mathrm{d}}{\mathrm{d}x} u_n \right\}, [\![v]\!] \right)_{\mathcal{E}_h^0} + (s_1 [\![u_n]\!], [\![v]\!])_{\mathcal{E}_h^0} \\ &\qquad + D_n(e_0) \frac{\mathrm{d}}{\mathrm{d}x} u_n(e_0) v_(e_0) - D_n(e_{N_k}) \frac{\mathrm{d}}{\mathrm{d}x} u_n(e_{N_k}) v(e_{N_k}) = (q_n, v)_{\mathcal{I}_h},\ \forall v \in \mathrm{H}^1(\mathcal{I}_h)\,, \end{aligned}$$

where we have used the boundary conditions $u(e_0) = 0$ and $u(e_{N_k}) = 0$. We notice that this formulation of the problem is the same as the one obtained in [28] for the neutron diffusion

equation with zero flux boundary conditions. The notation for the d- and $(d-1)$-measures of the functions, that for our one-dimensional problem corresponds to integrals over the elements in $\mathcal{I}_h$ and the evaluation at the elements in $\mathcal{E}_h$, stands as follows

$$(f,g)_{\mathcal{I}_h} = \sum_{I_k \in \mathcal{I}_h} (f,\ g)_{I_k} = \sum_{I_k \in \mathcal{I}_h} \int_{I_k} f(x)g(x)\,\mathrm{d}x\,, \quad (f,g)_{\mathcal{E}_h} = (f,g)_{\mathcal{E}_h^0} + (f,g)_{\mathcal{E}_h^\partial}$$
$$(f,g)_{\mathcal{E}_h^0} = \sum_{e \in \mathcal{E}_h^0} (f,\ g)_e = \sum_{e \in \mathcal{E}_h^0} f(e)g(e)\,, \quad (f,g)_{\mathcal{E}_h^\partial} = \sum_{e \in \mathcal{E}_h^\partial} (f,\ g)_e = f(e_0)g(e_0) + f(e_{N_k})g(e_{N_k})\,.$$

This formulation is also called Incomplete Interior Penalty Galerkin method (IIPG). A more detailed description of the different operators for higher dimensions can be found in [29]. Different formulations have also been proposed in [30] and [31], where the scheme is consistent with a transport formulation within the strategy of synthetic diffusion acceleration. The homogenization process and the inclusion of the discontinuity factors in the finite element method formulation is discussed in the next section.

3. Homogenization strategy

Numerically solving the neutron transport equation is challenging due to the heterogeneity of the domain at different scales, together with the complexity of the cross sections at fine scales and their energy dependence. A common strategy to circumvent these problems consists in using a two-stage calculation procedure, where the transport equation is solved accurately in single domains with proper assumptions regarding the boundary conditions, and these solutions are connected with each other through a full domain calculation with a homogenized equation. This approach is justified because of two main reasons: first, the solution domain shows a pattern with similar substructures repeated periodically and a subdomain with appropriate boundary conditions can be calculated in a stand-alone manner providing a good representation of the behaviour at fine scales. Secondly, homogenizing these substructures reduces the angular dependence of the solution at the coarser scale, where the problem now is well represented by a diffusion-like operator.

For this approach to be valid, we require the domain to be truly periodic, what is not the case for most of the problems. Nevertheless, almost periodic domains still provide accurate homogenization parameters. However there are situation where this assumption is far from being satisfied. In this scenario, the homogenization process is corrected with extra parameters that mitigate the effect of the heterogeneity and reduce the error due to wrong homogenization parameters [4, 3].

3.1. Homogenization of cross sections

In order to simplify the notation here, the transport equation to be homogenized is considered in its mono-energetic formulation. Equation (1), using expansions (3) and (4), the orthogonality relations of the Legendre polynomials and the addition theorem of the associated Legendre functions, can be rewritten as [10]

$$\left(\mu\frac{\mathrm{d}}{\mathrm{d}x} + \Sigma_t(x)\right)\psi(x,\mu) = \sum_{l=0}^{L} \frac{2l+1}{2} P_l(\mu)\Sigma_{sl}(x)\phi_l(x) + \frac{1}{\lambda}\chi(x)\nu\Sigma_f(x)\phi_0(x)\,, \tag{24}$$

and the SP_N approximation (6) is rewritten as

$$\frac{\mathrm{d}}{\mathrm{d}x}\left(\frac{n}{2n+1}\phi_{n-1}+\frac{n+1}{2n+1}\phi_{n+1}\right)+\left(\Sigma_t(x)-\delta_{n\leq L}\Sigma_{sn}(x)\right)\phi_n=\frac{\delta_{n,0}}{\lambda}\chi(x)\nu\Sigma_f(x)\phi_0,\quad n=0,\ldots,N, \tag{25}$$

where the lower and upper limits for the recurrence are $\phi_{-1}=\phi_{N+1}=0$. We consider the equations for the even and odd moments separately. Our target is to find a homogenized equation for even indices moments as follows

$$\frac{\mathrm{d}}{\mathrm{d}x}\left(\frac{n}{2n+1}\phi^h_{n-1}+\frac{n+1}{2n+1}\phi^h_{n+1}\right)+\left(\Sigma^h_t-\delta_{n\leq L}\Sigma^h_{sn}\right)\phi^h_n=\frac{\delta_{n,0}}{\lambda^h}\chi^h\nu\Sigma^h_f\phi^h_0,\quad n=0,\,2,\,\ldots,\,N-1, \tag{26}$$

which preserves local quantities over the smaller subdomains I_k, such as the average of the flux moments

$$\bar{\phi}_{k,n}:=\int_{I_k}\phi_n\,\mathrm{d}x=\int_{I_k}\phi^h_n\,\mathrm{d}x,\qquad n=0,\,2,\,\ldots,\,N-1, \tag{27}$$

which implies

$$\int_{I_k}u_n\,\mathrm{d}x=\int_{I_k}u^h_n\,\mathrm{d}x,\qquad n=0,\,2,\,\ldots,\,N-1, \tag{28}$$

and preserves the eigenvalue $\lambda^h=\lambda$ of the original problem, using piecewise constant cross sections in the subdomains. Moreover, we introduce the concepts of *High Order* (HO) and *Low Order* (LO) operators, meaning that different approximations can be used to solve the equations at different scales, where an HO operator is more accurate using more functions to represent space, angle and energy, but more expensive in computational terms. A LO operator has lower accuracy in space, angle and energy, but is computationally less expensive. Thus, when we talk about a solution of the original problem, this should be obtained with a HO solver, while the solution of the homogenized problem is obtained by a LO solver. Later on we will see that the homogenization parameters are tailored for the LO solver that is used to solve the homogenized equation.

A common strategy to obtain the homogenized parameters consists of integrating the original and the homogenized equations over each spatial subdomain, to obtain

$$\begin{aligned}\int_{I_k}\frac{\mathrm{d}}{\mathrm{d}x}\left(\frac{n}{2n+1}\phi_{n-1}+\frac{n+1}{2n+1}\phi_{n+1}\right)\mathrm{d}x+\int_{I_k}\left(\Sigma_t(x)-\delta_{n\leq L}\Sigma_{sn}(x)\right)\phi_n(x)\,\mathrm{d}x\mathrm{d}\mu\,\mathrm{d}x\\ =\frac{\delta_{0,n}}{\lambda}\int_{I_k}\chi(x)\nu\Sigma_f(x)\phi_0(x)\,\mathrm{d}x,\end{aligned} \tag{29}$$

$$\begin{aligned}\int_{I_k}\frac{\mathrm{d}}{\mathrm{d}x}\left(\frac{n}{2n+1}\phi^h_{n-1}+\frac{n+1}{2n+1}\phi^h_{n+1}\right)\mathrm{d}x+\left(\Sigma^h_t-\delta_{n\leq L}\Sigma^h_{sn}\right)\int_{I_k}\phi^h_n(x)\,\mathrm{d}x\mathrm{d}\mu\,\mathrm{d}x\\ =\frac{\delta_{0,n}}{\lambda^h}\chi^h\nu\Sigma^h_f\int_{I_k}\phi^h_0(x)\,\mathrm{d}x.\end{aligned} \tag{30}$$

Now we force equations (29) and (30) to be equal term by term, as follows

$$\int_{I_k} \frac{\mathrm{d}}{\mathrm{d}x}\left(\frac{n}{2n+1}\phi_{n-1} + \frac{n+1}{2n+1}\phi_{n+1}\right)\mathrm{d}x = \int_{I_k} \frac{\mathrm{d}}{\mathrm{d}x}\left(\frac{n}{2n+1}\phi^h_{n-1} + \frac{n+1}{2n+1}\phi^h_{n+1}\right)\mathrm{d}x\,, \tag{31}$$

$$\int_{I_k} \left(\Sigma_t(x) - \delta_{n\leq L}\Sigma_{sn}(x)\right)\phi_n(x)\,\mathrm{d}x = \left(\Sigma^h_t - \delta_{n\leq L}\Sigma^h_{sn}\right)\int_{I_k}\phi^h_n(x)\,\mathrm{d}x\,, \tag{32}$$

$$\frac{\delta_{0,n}}{\lambda}\int_{I_k}\frac{\chi(x)}{2}\nu\Sigma_f(x)\phi_0(x)\,\mathrm{d}x = \frac{\delta_{0,n}}{\lambda^h}\chi^h\nu\Sigma^h_f\int_{I_k}\phi^h_0(x)\,\mathrm{d}x\,, \tag{33}$$

in order to ensure that the solution of the homogenized equation reproduces the averages quantities of the heterogeneous solution in terms of reaction rates. We can see that using equation (27) to preserve average flux moments, and imposing $\lambda = \lambda^h$, we obtain from equation (33) that the homogenized fission cross section is defined by

$$\chi^h\nu\Sigma^h_f = \frac{\int_{I_k}\chi(x)\nu\Sigma_f(x)\phi_0(x)\,\mathrm{d}x}{\int_{I_k}\phi^h_0(x)\,\mathrm{d}x} = \frac{\int_{I_k}\chi(x)\nu\Sigma_f(x)\phi_0(x)\,\mathrm{d}x}{\bar{\phi}_{k,0}(x)}\,, \tag{34}$$

and because the homogenized solution does not appear in this expression, we say that the homogenized fission cross section is independent of the LO solver. We apply the same procedure to the scattering term in equation (32) to obtain

$$\left(\Sigma^h_t - \delta_{n\leq L}\Sigma^h_{sn}\right) = \frac{\int_{I_k}\left(\Sigma_t(x) - \delta_{n\leq L}\Sigma_{sn}(x)\right)\phi_n(x)\,\mathrm{d}x}{\int_{I_k}\phi^h_n(x)\,\mathrm{d}x} = \frac{\int_{I_k}\left(\Sigma_t(x) - \delta_{n\leq L}\Sigma_{sn}(x)\right)\phi_n(x)\,\mathrm{d}x}{\bar{\phi}_{k,n}(x)}\,. \tag{35}$$

But this definition of the homogenized cross section could produce non physical values, due to the fact that the denominator in the equation is not necessarily positive for all moments, $\bar{\phi}_n(x)$. This problem is exposed in [3], where the proposed solution consists in using the zero moment homogenized flux for the denominator, obtaining

$$\left(\Sigma^h_t - \delta_{n\leq L}\Sigma^h_{sm}\right) = \frac{\int_{I_k}\left(\Sigma_t(x) - \delta_{n\leq L}\Sigma_{sn}(x)\right)\phi_n(x)\,\mathrm{d}x}{\bar{\phi}_{k,0}(x)}\,. \tag{36}$$

Moreover, this approximation is exact for isotropic scattering problems because only zero order is considered for the homogenized cross section, and the error due to the change in the formula is preferred to the non-physical values obtained with negative or almost zero flux moments. We notice that the homogenized scattering cross section is also independent of the LO solver.

Last, we must deal with equation (31) involving the streaming terms in order to obtain a completely equivalent homogenized formulation. We integrate by parts equation (31) to obtain

$$\left[\frac{n}{2n+1}\phi_{n-1} + \frac{n+1}{2n+1}\phi_{n+1}\right]_{I_k} = \left[\frac{n}{2n+1}\phi^h_{n-1} + \frac{n+1}{2n+1}\phi^h_{n+1}\right]_{I_k}\,, \quad n = 0,\, 2,\, \ldots,\, N-1, \tag{37}$$

where $[f(x)]_{I_k} = f(x_k) - f(x_{k-1})$. Because it must happen for all odd indices, and we use the closures $\phi_{-1} = \phi_{N+1} = 0$, this is equivalent to ask for

$$[\phi_n]_{I_k} = [\phi^h_n]_{I_k}\,, \quad n = 1,\, 3,\, \ldots,\, N, \tag{38}$$

In order to continue, we want to express the odd moments in terms of the even ones. In order to do this, we go back to equation (25) and consider the odd fluxes. For odd indices the source term is zero because of the isotropic representation of the fission term (only exists for the zero moment), so the odd fluxes satisfy the following equations

$$\phi_n = -\frac{1}{(\Sigma_t(x) - \delta_{n\leq L}\Sigma_{sn})}\frac{\mathrm{d}}{\mathrm{d}x}\left(\frac{n}{2n+1}\phi_{n-1} + \frac{n+1}{2n+1}\phi_{n+1}\right), \quad n = 1, 3, \ldots, N, \tag{39}$$

that can be rewritten, using the definition of the diffusion-like coefficient and the change of variables (10), as follows

$$\phi_{n+1} = -D_n\frac{\mathrm{d}}{\mathrm{d}x}u_n, \quad D_n = \frac{1}{(2n+3)\,(\Sigma_t - \delta_{n\leq L}\Sigma_{sn})}, \quad n = 0, 2, \ldots, N-1. \tag{40}$$

Equation (38) will be satisfied if the heterogeneous and the homogeneous odd fluxes are equal pointwise at the interfaces, or average-wise for dimensions higher that 1. In terms of the even fluxes it reads as

$$-D_n\frac{\mathrm{d}}{\mathrm{d}x}u_n = -D_n^h\frac{\mathrm{d}}{\mathrm{d}x}u_n^h, \quad n = 0, 2, \ldots, N-1.$$

For clarification, we notice that in the special case of $N = 1$, the original equation is the neutron diffusion equation, and the previous expression takes the form of preserving the neutron current, J, at the interfaces by

$$J := -D_0\frac{\mathrm{d}}{\mathrm{d}x}\phi_0 = -D_0^h\frac{\mathrm{d}}{\mathrm{d}x}\phi_0^h := J^h.$$

The main problem is that this condition must be satisfied on the two boundaries of each of the K subdomains for one-dimension, for each of the $N/2$ even fluxes for each energy group, i.e. $K\times N\times G$ restrictions, but there is only one degree of freedom per subdomain, per even moment and per energy group, i.e. $K\times N/2\times G$ degrees of freedom, that can be tuned to force this situation, i.e., the coefficients D_{n-1}^h. Thus, we have more restrictions than degrees of freedoms and this can not be satisfied. Instead, we are going to use some extra parameters, called discontinuity factors, that add some extra degrees of freedom in order to recover some physical properties of the solution and minimize the homogenization error.

3.2. Discontinuity factors for the Simplified P_N

In the generalized equivalence theory [4], which is an extension of Koebke's homogenization method [5], flux discontinuity factors (DFs) are introduced in the neutron diffusion theory and they improve the homogenization strategy stated before. In this theory, for a given node e limiting two adjacent homogenized subdomains, the energy-dependent discontinuity factors are defined as interface constants f_e^-, f_e^+, such that the scalar flux, ϕ_0, satisfies the following condition

$$f_e^-\phi_0^{h-}(e) = f_e^+\phi_0^{h+}(e), \tag{41}$$

where ϕ_0^{h-} and ϕ_0^{h+} are the lateral limits of the homogenized scalar flux viewed from the two different subdomains sharing this node. A possible definition of these discontinuity factors is

$$f_e^- = \frac{\phi_0^-(e)}{\phi_0^{h-}(e)}, \qquad f_e^+ = \frac{\phi_0^+(e)}{\phi_0^{h+}(e)}, \tag{42}$$

so continuity for the heterogeneous reconstructed zero-th order flux is enforced [4].

The angular flux in one-dimensional geometries, $\psi(x,\mu)$, can be projected onto the different diffusive moments of the SP_N equations, u_n. Then, a homogeneous problem must be solved in the homogenized subdomain using odd reference flux moments as boundary conditions to calculate the homogeneous even flux moments.

To calculate the discontinuity factors for the SP_N equations in the subdomain edge e, equation (42) can be extended to

$$f^{+}_{n,e} = \frac{u^{+}_{n}(e)}{u^{h+}_{n}(e)}\,, \qquad f^{-}_{n,e} = \frac{u^{-}_{n}(e)}{u^{h-}_{n}(e)}\,, \qquad \text{for } n = 0,\, 2,\, \ldots,\, N-1\,, \tag{43}$$

where u^{-}_{n} and u^{+}_{n} are the left and right extremes of the reference heterogeneous diffusive moments defined in equation (10), extracted from the transport solution and u^{h-}_{n} and u^{h+}_{n} are the left and right extremes of the homogeneous diffusive moments calculated with the SP_N approximation in the homogenized region. Thus, for a given node e shared by two adjacent homogenized regions, for the different moments we have the relationship

$$f^{-}_{n,e}\, u^{h-}_{n}(e) = f^{+}_{n,e}\, u^{h+}_{n}(e)\,, \text{for } n = 0,\, 2,\, \ldots,\, N-1\,. \tag{44}$$

It is worth to notice that the values of the homogenized solution appear explicitly in equation (44), and thus, the values of the discontinuity factors will depend on the homogenized solution, which depends on the LO solver. Thus, the discontinuity factors depend on the LO solver that is going to be used when solving the homogenized equation.

At this point we need the value of the heterogeneous and homogeneous flux moments, $u_n(x)$ and $u^{h}_{n}(x)$ respectively, to generate the homogenized cross sections and the discontinuity factors. Since the full heterogeneous solution is not known, these values must be determined by calculating each heterogeneous subdomain separately with a high order transport operator. These calculations are performed for a *reference problem* [3] whose solution is close enough to the solution that would be obtained if the entire heterogeneous system was calculated.

Usually, the reference problem is an isolated assembly with reflective boundary conditions. Then, the assembly homogenized cross sections are generated with assembly heterogeneous flux from the reference problem. The homogeneous flux is the solution of the reference homogeneous assembly with reflective boundary conditions and using the assembly homogenized cross sections. We can calculate Assembly Discontinuity Factors (ADFs) dividing the heterogeneous flux by the homogeneous flux. A scheme of the problems solved to calculate the ADFs is shown in Figure 1a. It must be noted that for a homogeneous reflective assembly, as the homogeneous reference problem, the fluxes are spatially constant and all the spherical harmonics expansion terms are zero except the first one. In this work, for homogenization at assembly level, the discontinuity factors for the moments greater than 0 are arbitrarily set to 1.0 .

Another possibility is to use the assembly heterogeneous results to compute pin homogenized parameters. In this way, we solve a homogeneous pin problem using the cross sections and current boundary conditions for the isolated heterogeneous assembly problem. Then, the Pin Discontinuity Factors (PDFs) are calculated by the ratio of the reference pin boundary flux values and the homogeneous reference problem boundary flux values. This procedure is schematised in Figure 1b.

Finally, the heterogeneous flux calculated for the whole reactor can be used to generate reference cross sections and appropriate current boundary conditions. With the global k_{eff} and these cross sections the homogeneous flux can be generated in a particular region considered here as

an assembly or a pin. Then, Reference Discontinuity Factors (RDFs) are generated using equation (43). This strategy corresponds to Figure 1c. This technique provides exact homogenized parameters, but it requires the solution of the whole heterogeneous problem to generate the homogenized parameters, what makes it of no practical sense. However, it is used here to verify that the discontinuity factors technique is successfully implemented within the interior penalty finite element method (IP-FEM).

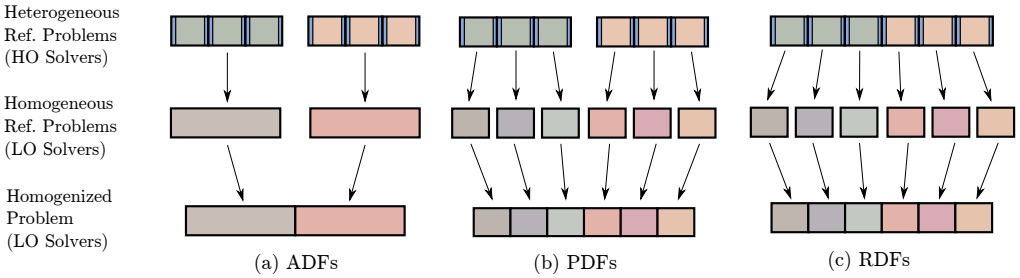

Figure 1: Scheme of homogenization strategies. The LO solvers for the *Homogeneous Ref. Problems* and for the *Homogenized problem* must be the same, due to the dependence of the discontinuity factors on the LO solver, at least for PDFs and RDFs (for ADFs the fluxes are constant and the solver used does not matter).

3.3. IP-FEM with discontinuity factors

In this case, the reference situation is one assembly or a pin with suitable boundary conditions. Thus, the continuity condition for the flux will be forced to be discontinuous as in equation (44). This type of interface conditions leads to a slightly different problem from the one stated by equations (18), (19) and (20), i.e., the problem with discontinuity factors is of the form

$$-\frac{\mathrm{d}}{\mathrm{d}x}D_n\frac{\mathrm{d}}{\mathrm{d}x}u_n + \Sigma_n u_n = q_n \quad \text{in each } I_k \in \mathcal{I}_h, \tag{45}$$

$$[\![u_n(e)]\!]_f = 0 \quad \text{on each } e \in \mathcal{E}_h, \tag{46}$$

$$\left[\!\!\left[D_n\frac{\mathrm{d}}{\mathrm{d}x}u_n(e) \right]\!\!\right] = 0 \quad \text{on each } e \in \mathcal{E}_h^0. \tag{47}$$

where the new jumps $[\![\cdot]\!]_f$ are defined as follows

$$\begin{aligned}
[\![u_n]\!]_f &= f^-_{n,e}\,\mathbf{n}^- u^-_n + f^+_{n,e}\,\mathbf{n}^+ u^+_n = f^-_{n,e}\,u^-_n - f^+_{n,e}\,u^+_n, \text{ on } e \in \mathcal{E}_h^0, \\
[\![u_n]\!]_f &= \begin{cases} f^-_{n,e_0}\,\mathbf{n}^+ u^+_n(e_0) & = -f^-_{n,e_0}\,u^+_n(e_0) \\ f^+_{n,e_{N_k}}\,\mathbf{n}^- u^-_n(e_{N_k}) & = +f^+_{n,e_{N_k}}\,u^-_n(e_{N_k}) \end{cases}, \text{ on } e \in \mathcal{E}_h^\partial,
\end{aligned} \tag{48}$$

where $f^+_{n,e}$ is generally different from $f^-_{n,e}$ for a particular edge e and even moment n, defining the jumps imposed to the solution, u_n. A scheme to approximate the problem defined by equations (45), (46) and (47), has been implemented in an IP-FEM using a formulation based on equation (22) as follows

$$\left(D_n\frac{\mathrm{d}}{\mathrm{d}x}u_n, \frac{\mathrm{d}}{\mathrm{d}x}v_n\right)_{\mathcal{I}_h} + (\Sigma_n u_n, v_n)_{\mathcal{I}_h} - \left(\left\{D\frac{\mathrm{d}}{\mathrm{d}x}u_n\right\}, [\![v_n]\!]\right)_{\mathcal{E}_h} + \left(s_1\,[\![u]\!]_f\,, [\![v_n]\!]\right)_{\mathcal{E}_h} = (q_n, v_n)_{\mathcal{I}_h}, \tag{49}$$

following analogous steps to the ones presented in [28] for the neutron diffusion equation.

4. Numerical Results

To study the performance of the homogenization method exposed above, two different one-dimensional reactor configurations based on the C5G7 benchmark [32] are defined. The first configuration is comprised of two assemblies and the second configuration has five assemblies of 21.42 cm wide with reflective boundary conditions as Figure 2 shows. Each assembly consists of 17 pins of 1.26 cm wide, each pin is made of a layer of nuclear fuel of 1.08 cm, surrounded by a thin layer of water of 0.09 cm. The particular composition of each one of the assemblies can be found in Figure 3 and the pins composition is presented in Figure 4. Seven energy group cross sections for every material can be found in reference [32].

(a) Configuration 1

(b) Configuration 2

Figure 2: Reactor configurations definition.

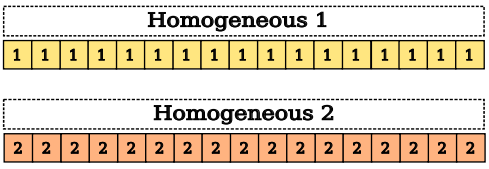

(a) Assemblies for Configuration 1

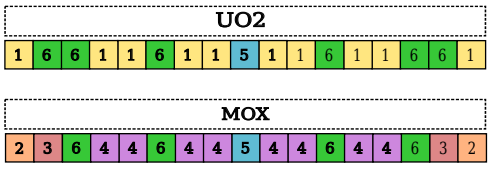

(b) Assemblies for Configuration 2

Figure 3: Assemblies composition. Each pin is defined in Figure 4. Pin types 1, 2, 3 and 4 contain nuclear fuel while pin types 5 and 6 do not contain fissile materials.

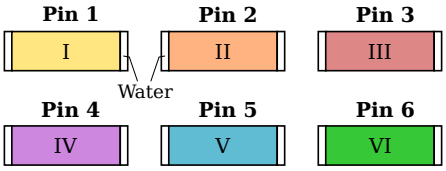

Figure 4: Pins composition. Material I is UO_2 fuel, material II is 4.3% MOX, material III is 7.0% MOX, material IV is 8.7% MOX, material V is the fission chamber and material VI is the guide tube.

Different strategies for the homogenization of the two reactor configurations are compared in this work. These strategies are presented in Table 2. The reason for including RXS (reference cross sections without discontinuity factors) is to show that using better homogenized cross

section does not correct the homogenization error alone, thus being advantageous the use of discontinuity factors even if the cross sections are just an approximation.

Table 2: Acronyms used for the different homogenization strategies.

No DFs	Problem without DFs and assembly homogenized cross sections.
RXSs	Problem without DFs and reference homogenized cross sections.
ADFs	Problem with assembly DFs and assembly homogenized cross sections.
PDFs	Problem with pin DFs and pin homogenized cross sections, they are calculated from an isolated assembly problem.
RDFs	Problem with reference DFs and reference homogenized cross sections.

To compare the results, neutronic power averaged assembly and neutronic power averaged pin errors are condensed using the root mean square (RMS) of the relative errors as defined in equation (50),

$$\mathrm{RMS} = \sqrt{\frac{1}{L_t}\sum_i L_i \left(\frac{P_i - P_i^*}{P_i^*}\right)^2}\ , \tag{50}$$

where P_i and P_i^* represent the homogeneous and the heterogeneous reference, respectively, averaged neutronic power in the region i (this region can be an assembly or a pin). L_i represents the length of the region i and L_t is the total length of the reactor. The averaged power in region i is defined as

$$P_i = \frac{1}{L_i}\int_{L_i}\sum_{g=1}^{G}\Sigma_f^g\phi_0^g\,\mathrm{d}x. \tag{51}$$

In the same way, the maximum relative error for the scalar flux, ϕ_0 is defined as

$$\epsilon = \max\left(\frac{\left|\phi_0 - \phi_0^*\right|}{\phi_0^*}\right), \tag{52}$$

where ϕ_0 and ϕ_0^* represent the homogeneous and the heterogeneous reference, respectively, scalar fluxes. The eigenvalue absolute error is calculated in pcm as

$$\Delta k_{\mathrm{eff}} = 10^5\left|k_{\mathrm{eff}} - k_{\mathrm{eff}}^*\right|\ , \tag{53}$$

where k_{eff} and k_{eff}^* represent the homogeneous and the heterogeneous reference, respectively, multiplicative factors. The transport reference solution is calculated with a discrete ordinates code using a S_{96} approximation where the solution is fully converged. The transport reference results are also used to compute reference homogenized cross sections and reference discontinuity factors. The same code using a discrete ordinates approximations of order 96 is used to calculate isolated assembly heterogeneous fluxes to be able to calculate assembly and pin homogenization parameters.

4.1. Configuration 1

The reactor named configuration 1 is composed of two different assemblies. Each assembly is formed by 17 equal pins. Figures 5a and 5b show the heterogeneous fluxes for the same transport

approximations for $g = 1$ and $g = 7$ energy groups. Figures 5c and 5d show the relative errors for these energy groups. Looking at Figure 5a for the flux for $g = 1$, and its relative error in Figure 5c, we see that the error is mostly due to the the fact that the lower order approximations SP_1, SP_3 and SP_5 do not capture the local behaviour of the solution in regions with water, where the flux is lower than in fuel regions for fast groups (low values of g). The same problem occurs when looking at the behaviour for $g = 7$ in Figures 5b and 5d, but this time because the flux is underestimated in the region with water, where the flux is larger than in regions with fuel for slow groups (high values of g). This behaviour is typical. Moreover, we also observe that the relative error is much bigger for $g = 7$ than for $g = 1$ (around one order of magnitude), but this is mainly due to the fact that the value of the flux is smaller (around one order of magnitude), and this means that the absolute value of the error is similar (of the same order). This effect is enhanced by the fact that strong heterogeneity in the cross sections in the thermal groups ($g > 5$) result in more heterogeneous thermal fluxes.

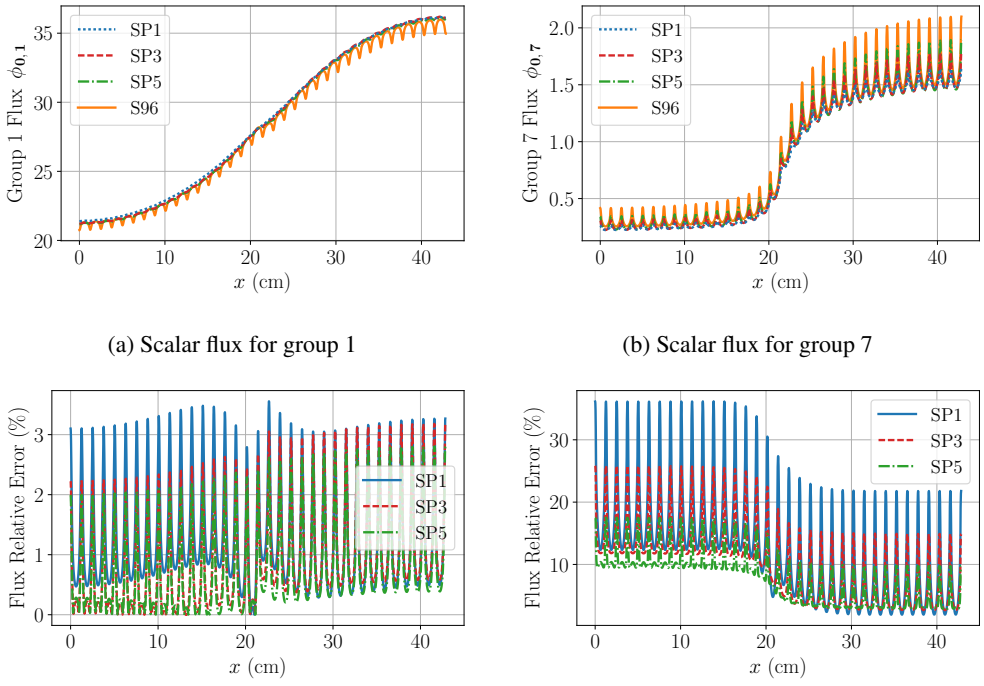

(a) Scalar flux for group 1

(b) Scalar flux for group 7

(c) Relative error for group 1

(d) Relative error for group 7

Figure 5: Comparison of results for heterogeneous fluxes and the spatial distribution of the relative error in the scalar flux for Configuration 1 test.

Table 3 shows a comparison of the heterogeneous results for this reactor, without any homogenization, for different order of SP_N approximations to the neutron transport equation and different finite element polynomials degrees p. In this comparison, the different k_{eff} for the different approximations are provided together with the difference with respect to the reference results, as well as the Root Mean Square error for the neutronic power, and the maximum relative error

(pointwise) for the fluxes for groups $g = 1$ and $g = 7$. The results show that the problem is spatially converged for polynomials of fifth degree, so for now on, all calculations will be performed with $p = 5$. It must be noted that the relative errors are much larger for the thermal groups ($g > 3$), i.e., the relative error for the $g = 7$ flux is locally above 35% for SP_1, 25% for SP_3, and 15% for SP_5, as it has been explained before. Instead the pin averages power RMS errors are less than 0.4% for any of the approximations. The reason for this is that the regions with water do not produce power (because there is not fission there), so the error in these regions does not directly affect the RMS error in the power (neither assembly-wise nor pin-wise). Nevertheless, we can observe that the error in the k_{eff} is very big for these approximations (above 900 pcm for $N \leq 5$) because this global parameter is affected by errors in the water regions through the balance equations. Increasing the order of the angular approximation for SP_N affects mainly the value of the k_{eff} through better capturing of the behaviour in these regions.

Table 3: Comparison of heterogeneous results for Configuration 1.

Transport		**Eigenvalue**		**Power RMS**		**Flux Max. Rel. Error**	
Approx.	p	k_{eff}	Δk_{eff} (pcm)	Assembly (%)	Pin (%)	$g = 1$ (%)	$g = 7$ (%)
SP_1	1	0.90951	1 563	0.07	0.46	3.85	43.29
	3	0.90951	1 360	0.05	0.32	3.56	36.18
	5	0.91154	1 360	0.05	0.32	3.56	36.18
SP_3	1	0.91015	1 499	0.35	0.46	3.85	40.51
	3	0.91411	1 103	0.34	0.37	3.18	25.85
	5	0.91411	1 103	0.34	0.37	3.18	25.84
SP_5	1	0.91042	1 472	0.33	0.42	3.77	38.37
	3	0.91610	904	0.30	0.32	2.80	17.56
	5	0.91610	904	0.30	0.32	2.80	17.49
S_{96}		0.92514					

Table 4 shows the assembly-wise homogenization results for different SP_N approximations using different homogenization strategies defined in Table 2. At assembly level, the diffusion theory, SP_1, results are accurate enough and increasing the number of spherical harmonics does not provide better results. This behaviour is explained by the fact that the assemblies are large enough to provide precise average results with a LO solver such as the diffusion approximation, and the angular dependence does not have a strong effect average-wise for this size of the homogenized regions. However, reconstructed pin power results have RMS errors around 11%. This is explained by the assembly shape function (which is the heterogeneous power computed for an isolated assembly with reflexive boundary conditions) being inaccurate as it does not take into account influences of neighbouring assemblies. To improve these results a more sophisticated reconstruction method or pin homogenization strategy is necessary. We can also mention that using RXSs provide good results, even if no discontinuity factors are used. This is because the reconstruction has been done with the right shape for the local flux, which in practical reactor calculations is not available. Nevertheless, we observe that we must also use discontinuity factors together with the reference cross sections, RDFs, in order to completely reproduce the average values of the power and the k_{eff} of the original problem with a HO solver with the homogenized

problem and a LO solver.

Table 4: Comparison for assembly-wise homogenization results for Configuration 1.

Transport Approx.	**Homogenization Method**	**Eigenvalue**		**Power RMS**	
		k_{eff}	Δk_{eff} (pcm)	Assembly (%)	Pin (%)
SP_1	No DFs	0.92475	39	0.49	10.95
	ADFs	0.92547	33	0.10	10.90
	RXSs	0.92468	46	0.39	0.39
	RDFs	0.92514	0	0.00	0.00
SP_3	No DFs	0.92514	0	0.06	10.91
	ADFs	0.92583	69	0.52	10.88
	RXSs	0.92507	7	0.04	0.04
	RDFs	0.92514	0	0.00	0.00
SP_5	No DFs	0.92516	2	0.06	10.91
	ADFs	0.92585	71	0.53	10.88
	RXSs	0.92509	5	0.05	0.05
	RDFs	0.92514	0	0.00	0.00
Transport Reference		0.92514			

Last, pin-wise homogenization results are shown in Table 5. In this Table, we can observe a similar behaviour as for average-wise homogenization except that now the RMS error is reduced for pin-power averages. This is the main reason for using pin discontinuity factors. This comes from the choice of smaller domains for the homogenization and it requires that we correct the homogenization error at these scales. The RXSs and RDFs results behave analogously to the case of assembly-wise homogenization above.

4.2. Configuration 2

The reactor named as Configuration 2 is composed of five assemblies with reflexive boundary conditions. Each assembly is composed of 17 pins describing an usual nuclear arrangement. This test is built to be more heterogeneous than the previous one, to be able to test the different homogenization methods in more realistic conditions, since the composition of each assembly will not be completely homogeneous.

First we analyse the behaviour of the fluxes and the errors for different energy groups and different LO solvers (SP_1, SP_3, and SP_5) without spatial homogenization. Figures 6a and 6b present the heterogeneous scalar fluxes, ϕ_0^g, of the groups $g = 1$ and $g = 7$ for different transport approximations. Figures 6c and 6d show the relative errors for these low order angular approximations. We see a similar behaviour as the one observed in the previous problem. In this way, the relative errors are larger for thermal groups $g > 5$. than for fast groups $g < 5$. Again we observe that this effect is higher in the regions with water and now also in regions with materials 5 and 6, which represent strong absorbers or fission chambers where almost no fission occurs. Again, the LO solvers are unable to fully capture the behaviour of the HO solver (S_{96}) in these regions.

Table 5: Comparison for pin-wise homogenization results for Configuration 1.

Transport Approx.	**Homogenization Method**	**Eigenvalue**		**Power RMS**	
		k_{eff}	Δk_{eff} (pcm)	Assembly (%)	Pin (%)
SP_1	No DFs	0.92476	38	0.49	0.56
	PDFs	0.92547	33	0.10	0.44
	RXSs	0.92469	45	0.42	0.53
	RDFs	0.92514	0	0.00	0.00
SP_3	No DFs	0.92515	1	0.05	0.15
	PDFs	0.92531	17	0.11	0.15
	RXSs	0.92508	6	0.02	0.17
	RDFs	0.92514	0	0.00	0.00
SP_5	No DFs	0.92517	3	0.04	0.11
	PDFs	0.92533	19	0.12	0.17
	RXSs	0.92511	3	0.02	0.13
	RDFs	0.92514	0	0.00	0.00
Transport Reference		0.92514			

Table 6 shows a comparison of the heterogeneous results, without any homogenization, for SP_1, SP_3, and SP_5, approximations. This Table shows the same type of errors as Table 3. We can see the same behaviour, with larger point-wise flux maximum relative error for $g = 7$ than for $g = 1$, and large errors in the eigenvalue of the problem. We can also see that the average-wise error is larger for the power (pin-wise and assembly-wise), and that this error decreases when increasing the order of the LO solver. This suggests that for more realistic problems, there is actually a need of using LO solvers of slightly higher order for reducing both pin-wise and assembly-wise, RMS errors for average power.

Table 6: Comparison of heterogeneous results for Configuration 2.

Transport Approx.	**Eigenvalue**		**Power RMS**		**Flux Max. Rel. Error**	
	k_{eff}	Δk_{eff} (pcm)	Assembly (%)	Pin (%)	$g = 1$ (%)	$g = 7$ (%)
SP_1	1.11869	1 443	2.05	2.03	13.25	36.77
SP_3	1.12290	1 022	1.30	1.17	8.18	23.33
SP_5	1.12649	663	0.75	0.68	5.04	13.83
S_{96}	1.13312					

Table 7 shows the assembly-wise homogenization results SP_1, SP_3 and SP_5 approximations using the different strategies of homogenization defined in Table 2. As it occurs for reactor Configuration 1, for reactor Configuration 2 the computations at assembly level using ADFs, by means of the diffusion theory, SP_1, are accurate enough and increasing the number of spherical harmonics in the transport approximation does not provide better results. In this case, the introduction of assembly discontinuity factors improves the obtained solution in terms of eigenvalue error and assembly averaged neutronic error, while the pin-wise RMS error remains high, even

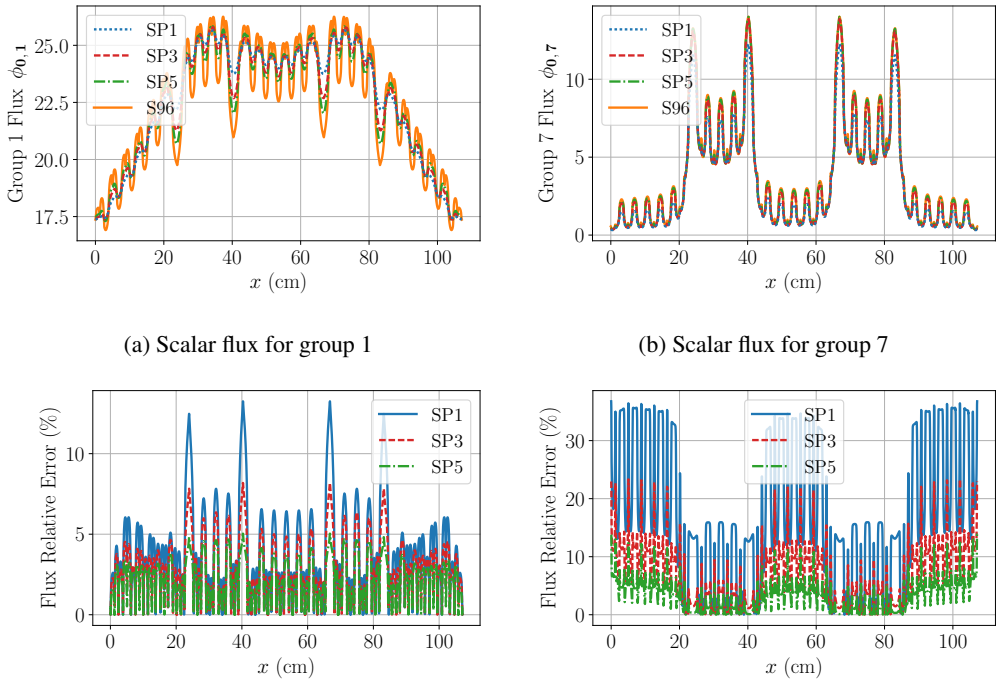

(a) Scalar flux for group 1

(b) Scalar flux for group 7

(c) Relative error for group 1

(d) Relative error for group 7

Figure 6: Comparison of results for heterogeneous fluxes and the spatial distribution of the relative error in the scalar flux for Configuration 2 test.

if the order of the LO solver is increased up to SP_5.

Results for pin-wise homogenization are shown in Table 8. We see that the use of pin-wise homogenization provides more accurate results, both in assembly and pin averaged power, specially if the proposed pin discontinuity factors are used. Increasing the number of spherical harmonics, N, reduces the eigenvalue error and pin averaged power errors because at pin scale the angular dependence is relevant. In this way, if the proposed pin discontinuity factors are used, the eigenvalue error can be reduced to 38 pcm and less than 1% in pin averaged power error results if one uses SP_5 approximation.

Table 7: Comparison for assembly-wise homogenization results for Configuration 2.

Transport Approx.	**Homogenization Method**	**Eigenvalue**		**Power RMS**	
		k_{eff}	Δk_{eff} (pcm)	Assembly (%)	Pin (%)
SP_1	No DFs	1.13462	150	1.20	14.82
	ADFs	1.13334	22	1.52	14.95
	RXSs	1.13368	56	3.16	2.55
	RDFs	1.13312	0	0.00	0.0
SP_3	No DFs	1.13613	301	3.54	15.00
	ADFs	1.13392	80	0.95	14.89
	RXSs	1.13421	109	3.70	2.97
	RDFs	1.13312	0	0.00	0.00
SP_5	No DFs	1.13618	306	3.55	15.00
	ADFs	1.13398	86	0.94	14.89
	RXSs	1.13426	114	3.71	2.98
	RDFs	1.13312	0	0.00	0.00
Transport Reference		1.13312			

Table 8: Comparison for pin-wise homogenization results for Configuration 2.

Transport Approx.	**Homogenization Method**	**Eigenvalue**		**Power RMS**	
		k_{eff}	Δk_{eff} (pcm)	Assembly (%)	Pin (%)
SP_1	No DFs	1.12458	854	1.66	1.66
	PDFs	1.13331	19	0.46	1.43
	RXSs	1.12436	876	1.64	1.67
	RDFs	1.13312	0	0.00	0.00
SP_3	No DFs	1.12795	517	1.32	1.20
	PDFs	1.1335	55	0.89	0.92
	RXSs	1.12775	537	1.31	1.18
	RDFs	1.13312	0	0.00	0.00
SP_5	No DFs	1.13053	259	1.03	0.94
	PDFs	1.1335	38	0.76	0.78
	RXSs	1.13033	279	1.02	0.93
	RDFs	1.13312	0	0.00	0.00
Transport Reference		1.13312			

5. Conclusions

An extension of the generalized equivalence theory for the Simplified P_N equations in one-dimensional geometries has been developed in this work using a finite element method. This extension proposes pin discontinuity factors for every even flux moment of the spherical harmonics approximation calculated from an isolated assembly transport calculation and the use of SP_3 or SP_5 approximations to the neutron transport equation for accurate reactor calculations. An interior penalty finite element method has been presented to discretize and solve the problem using discontinuity factors.

Numerical results show that low order spherical harmonics approximations cannot reproduce accurately sub-pin heterogeneities when solving for the whole domain. This strongly affects the approximation of the largest eigenvalue of the problem. In order to improve the approximation for the largest eigenvalue while keeping the computations efficient, the problem can be solved using a homogenization process with two different solvers at two different scales. In this way, assembly discontinuity factors correct some of the errors introduced during the homogenization process, and it produces acceptable eigenvalue and assembly averaged results using diffusion theory, even if they do not reconstruct precise pin averaged results. The proposed pin discontinuity factors produce accurate results for both pin and assembly averaged values without the use of reconstruction methods. The results show that pin-wise homogenization is a reliable methodology instead of the computationally expensive full-core heterogeneous calculations. Also, the homogenization methodology has been verified with the calculation of reference discontinuity factors, which fully reproduce average values with the homogenized problem. The extension of this work to multidimensional geometries using the simplified spherical harmonics method will be undertaken in the future.

Acknowledgements

The work has been partially supported by the spanish Ministerio de Economía y Competitividad under projects ENE 2014-59442-P and MTM2014-58159-P, the Generalitat Valenciana under the project PROMETEO II/2014/008 and the Universitat Politècnica de València under the project FPI-2013. The work has also been supported partially by the Swedish Research Council (VR-Vetenskapsrådet) within a framework grant called DREAM4SAFER, research contract C0467701.

References

[1] E. E. Lewis, W. F. Miller, Computational methods of neutron transport, John Wiley and Sons, Inc., New York, NY, 1984.

[2] A. Vidal-Ferrandiz, R. Fayez, D. Ginestar, G. Verdú, Solution of the Lambda modes problem of a nuclear power reactor using an hp finite element method, Annals of Nuclear Energy 72 (2014) 338–349, ISSN 0306-4549, doi: 10.1016/j.anucene.2014.05.026.

[3] R. Sanchez, Assembly homogenization techniques for core calculations, Progress in Nuclear Energy 51 (2009) 14–31, doi:10.1016/j.pnucene.2008.01.009.

[4] K. Smith, Assembly homogenization techniques for light water reactor analysis, Progress in Nuclear Energy 17 (1986) 303 – 335, ISSN 0149-1970, doi:10.1016/0149-1970(86)90035-1.

[5] M. R. Wagner, K. Koebke, Progress in nodal reactor analysis, Atomkernenergie Kerntechnik. ANS topical meeting on advances in reactor computations; Salt Lake City, UT (USA) 43 (1983) 117–126.

[6] R. Sanchez, G. Dante, I. Zmijarevic, Diffusion Piecewise Homogenization via Flux Discontinuity Ratios, Nuclear Engineering and Technology 45 (2013) 707–720, doi:10.5516/NET.02.2013.518.

[7] T. J. Trahan, E. W. Larsen, Asymptotic, multigroup flux reconstruction and consistent discontinuity factors, Journal of Nuclear Science and Technology 52 (2015) 917–931.
[8] G. Allaire, Y. Capdeboscq, Homogenization of a spectral problem in neutronic multigroup diffusion, Computer methods in applied mechanics and engineering 187 (2000) 91–117.
[9] G. Allaire, G. Bal, Homogenization of the criticality spectral equation in neutron transport, ESAIM: Mathematical Modelling and Numerical Analysis 33 (4) (1999) 721–746.
[10] W. M. Stacey, Nuclear reactor physics, Wiley-VCH Verlag GmbH & Co. KGaA, ISBN 9783527611041, doi: 10.1002/9783527611041, 2007.
[11] E. W. Larsen, J. Morel, J. M. McGhee, Asymptotic derivation of the multigroup P_1 and simplified P_N equations with anisotropic scattering, Nuclear science and engineering 123 (1996) 328–342.
[12] T. Kozlowski, Y. Xu, T. J. Downar, D. Lee, Cell homogenization method for pin-by-pin neutron transport calculations, Nuclear science and engineering 169 (2011) 1–18.
[13] L. Yu, D. Lu, Y. A. Chao, The calculation method for SP_3 discontinuity factor and its application, Annals of Nuclear Energy 69 (2014) 14–24, ISSN 03064549, doi:10.1016/j.anucene.2014.01.032.
[14] L. Yu, Y.-A. Chao, A unified generic theory on discontinuity factors in diffusion, SP_3 and transport calculations, Annals of Nuclear Energy 75 (2015) 239–248.
[15] Y.-A. Chao, A new SPn theory formulation with self-consistent physical assumptions on angular flux, Annals of Nuclear Energy 87 (2016) 137–144.
[16] Y.-A. Chao, A new and rigorous SP_N theory for piecewise homogeneous regions, Annals of Nuclear Energy 96 (2016) 112–125.
[17] A. Yamamoto, T. Sakamoto, T. Endo, Discontinuity Factors for Simplified P3 Theory, Nuclear Science and Engineering 183 (2016) 39–51, doi:10.13182/NSE15-102.
[18] B. Turcksin, J. C. Ragusa, W. Bangerth, Goal-oriented h-adaptivity for the multigroup SPn equations, Nuclear Science and Engineering 165 (2010) 305–319.
[19] J. C. Ragusa, Application of h-, p-, and hp-Mesh Adaptation Techniques to the SP_3 Equations, Transport Theory and Statistical Physics 39 (2010) 234–254.
[20] Y. Zhang, J. C. Ragusa, J. E. Morel, Iterative performance of various formulations of the SP_N equations, Journal of Computational Physics 252 (2013) 558–572.
[21] E. M. Gelbard, Application of spherical harmonics methods to reactor problems, Tech. Rep., WAPD-BT-20. Bettis Atomic Power Laboratory, 1960.
[22] A. Henry, Nuclear-Reactor analysis, MIT Press, Cambridge, MA, USA, ISBN 9780262080811, 1975.
[23] R. Sanchez, On S_N-P_N Equivalence, Transport Theory and Statistical Physics 41 (2012) 418–447.
[24] P. S. Brantley, E. W. Larsen, The simplified P_3 approximation, Nuclear science and engineering 134 (2000) 1–21, doi:dx.doi.org/10.13182/NSE134-01.
[25] M. Capilla, C. Talavera, D. Ginestar, G. Verdú, A nodal collocation method for the calculation of the Lambda modes of the PL equations, Annals of Nuclear Energy 32 (2005) 1825 – 1853, ISSN 0306-4549.
[26] C. Hauck, R. McClarren, Positive P_N Closures, SIAM Journal on Scientific Computing 32 (2010) 2603–2626, doi:10.1137/090764918.
[27] S. P. Hamilton, T. M. Evans, Efficient solution of the simplified P_N equtations, Journal of Computational Physics 284 (2015) 155–170, ISSN 00219991, doi:10.1016/j.jcp.2014.12.014.
[28] A. Vidal-Ferràndiz, S. González-Pintor, D. Ginestar, G. Verdú, M. Asadzadeh, C. Demazière, Use of discontinuity factors in high-order finite element methods, Annals of Nuclear Energy 87, Part 2 (2016) 728 – 738, ISSN 0306-4549, doi:10.1016/j.anucene.2015.06.021.
[29] F. Brezzi, B. Cockburn, L. D. Marini, E. Süli, Stabilization mechanisms in discontinuous Galerkin finite element methods, Computer Methods in Applied Mechanics and Engineering 195 (2006) 3293–3310, ISSN 00457825, doi:10.1016/j.cma.2005.06.015.
[30] Y. Wang, J. C. Ragusa, Diffusion Synthetic Acceleration for High-Order Discontinuous Finite Element SN Transport Schemes and Application to Locally Refined Unstructured Meshes, Nuclear Science and Engineering 166 (2010) 145–166, ISSN 00295639, doi:10.13182/NSE09-46.
[31] B. Turcksin, J. C. Ragusa, Discontinuous diffusion synthetic acceleration for Sn transport on 2D arbitrary polygonal meshes, Journal of Computational Physics 274 (2014) 356–369, ISSN 00219991, doi:10.1016/j.jcp.2014.05.044.
[32] E. Lewis, M. Smith, N. Tsoulfanidis, G. Palmiotti, T. Taiwo, R. Blomquist, Benchmark specification for Deterministic 2-D/3-D MOX fuel assembly transport calculations without spatial homogenization (C5G7 MOX), Tech. Rep., NEA/NSC/DOC, 2001.

Appendix A. Boundary Conditions in SP_N

To approximate the vacuum boundary conditions, we shall consider Marshak's conditions [10]. These boundary conditions impose a restriction in the flux odd moments at each boundary, x_B, given by

$$\int_{\mu_{in}} P_n(\mu)\,\psi^g(x_B,\mu)\mathrm{d}\mu = 0, \qquad g = 1,\ 2,\ \ldots,\ G, \quad n = 1,\ 3,\ \ldots, N. \tag{A.1}$$

Expanding $\psi(L_t,\mu)$ using equation (3),

$$\int_{\mu_{in}} P_n(\mu) \sum_{n'=0}^{N} \frac{2n'+1}{2}\phi^g_{n'}(x_B,\mu)P_{n'}(\mu)\mathrm{d}\mu = 0, \quad g = 1,\ 2,\ \ldots,\ G, \quad n = 1,\ 3,\ \ldots, N. \tag{A.2}$$

Using the orthogonality relationship of Legendre polynomials and setting $N = 5$, the Marshak's boundary condition are,

$$\begin{aligned}
\frac{1}{2}\Phi_0 + \frac{5}{8}\Phi_2 - \frac{3}{16}\Phi_4 &= -\Phi_1,\\
-\frac{1}{8}\Phi_0 + \frac{5}{8}\Phi_2 - \frac{81}{128}\Phi_4 &= -\Phi_3,\\
\frac{1}{16}\Phi_0 - \frac{25}{128}\Phi_2 - \frac{81}{128}\Phi_4 &= -\Phi_5\,.
\end{aligned}$$

Applying the change of variables proposed in equation (10), the vacuum condition in the P_5 approximation can be applied as

$$-\hat{n}\,\mathbf{D}\frac{\mathrm{d}}{\mathrm{d}x}U(x_B) = \mathbf{B}U(x_B)\,, \tag{A.3}$$

where matrix $\mathbf{B}$ is given by the Kronecker product of matrix $\mathbf{b}$ by an $(G\times G)$ identity matrix,

$$\mathbf{B} = \mathbf{b}\otimes\mathbf{I}_{(G\times G)}\,, \qquad \mathbf{b} = \begin{pmatrix} \frac{1}{2} & -\frac{1}{8} & \frac{1}{16} \\ -\frac{1}{8} & \frac{7}{24} & -\frac{41}{384} \\ \frac{1}{16} & -\frac{41}{384} & \frac{407}{1920} \end{pmatrix}, \tag{A.4}$$

and $\hat{n}$ is the normal direction of the boundary, either 1 or -1 in one dimensional geometries.

On the other hand, reflective boundary conditions are imposed if all the flux odd moments are set to zero.

$$\phi^g_n(x_B) = 0, \qquad g = 1,\ 2,\ \ldots,\ G, \quad n = 1,\ 3,\ \ldots,\ N\,. \tag{A.5}$$

Thus, reflective boundary conditions are set imposing,

$$\frac{\mathrm{d}}{\mathrm{d}x}u^g_n(x_B) = 0, \qquad g = 1,\ 2,\ \ldots,\ G, \quad n = 0,\ 2,\ \ldots,\ N\,. \tag{A.6}$$

These treatments yield to $(N+1)/2$ equations in the boundary that effectively clauses the system. We note that both of these boundary conditions treatments contain asymmetric components when N is even. Thus, only odd sets of SP_N equations are considered. It must be noted that for each group the SP_N system of equations (15) is symmetric because the coefficients $\mathbf{c^{(m)}}$ and $\mathbf{B}$ are symmetric.